This article has been accepted for publication in a future issue of this journal, but has not been fully edited. Content may change prior to final publication. Citation information: DOI 10.1109/JLT.2019.2904560, Journal of Lightwave Technology

Fully distributed optical fiber strain sensor with 10^{-12} ε/√Hz sensitivity

Luís Costa, Hugo F. Martins, Sonia Martín-López, María R. Fernández-Ruiz and Miguel González-Herráez

***Abstract*— Advanced optical fiber reflectometry techniques enable spatially distributed measurements of true relative deformations over the length of a conventional optical fiber cable. This methodology is attractive for many applications ranging from intrusion monitoring to seismology. However, accurate quantification of the applied stimulus in general implies sophisticated implementations with poor sensitivity performance. Coherent reflectometry using chirped pulses is an appealing solution, as it provides fast dynamic strain measurements with a simple experimental deployment. Here, we analyze for the first time to our knowledge the lower performance bounds of this technique as a function of the signal-to-noise ratio of the acquired optical signal. We demonstrate that implementations realized so far have been limited by the temporal sampling used instead of the optical signal quality. Through post-processing interpolation approaches, we reach the performance limit for a given set of signal parameters, attaining unprecedented strain sensitivities (~10^{-12} ε/√Hz) for km-length distributed sensors in conventional single-mode fibers.**

***Index Terms*—Chirp modulation; Optical fiber applications; Optical time domain reflectometry; Phase noise; Remote sensing; Strain measurement; Vibration measurement**

I. Introduction

OPTICAL sensors have often shown to be capable of reaching ultra-high strain sensitivities. Successive attempts at approaching the fundamental noise introduced by thermodynamic vibrations within a fiber-optic medium have appeared in the literature, attaining remarkable strain sensitivities of 0.03×10^{-12} ε/√Hz at frequencies above 20 kHz, using a short (4.5 mm) Bragg grating interrogated via an ultra-stable laser source and a lock-in amplifier to reduce electrical noise [1], while previously a 130 mm Fabry-Perot fiber resonator reached sensitivities of ~0.35×10^{-12} ε/√Hz in the low frequency (Hz) range and ~0.22×10^{-12} ε/√Hz in the kHz range, by using a laser source stabilized against a quartz-oscillator phase-locked optical frequency comb [2]. Though highly encouraging, these record-breaking sensor designs present critical implementation shortcomings and stability requirements that restrain their use in most practical environments. Moreover, all these studies have been restricted to short gauge, point sensor implementations.

The field of sensing is currently receiving unprecedented attention from areas such as defense, energy and civil engineering, which are now recognizing the potential of endowing increasingly complex structures and materials with the ability to self-diagnose and react to environmental changes, leading to general increases in safety, production yields and considerable cost-savings in long term maintenance and inspection [3]. Distributed fiber optic alternatives arise as particularly attractive solutions, effectively replacing the need for hundreds or thousands of sensors and complex wiring schemes with a single optical fiber cable. The benefits come as lower cost-per-sensor in applications where multiple sensors are to be installed in a remote location, and limited intrusiveness of the sensing element in the host material in embedded applications (due to the lower number of ingress/egress points, lower total weight and smaller dimensions).

Distributed sensing is made possible by envisioning a single fiber as the data transmission and sensing element altogether, exploiting light-matter interactions at each position to retrieve information about the local fiber properties (e.g. temperature [4]–[8] and strain [6]–[9]). Usually, this consists in pairing natural elastic and inelastic backscattering phenomena [10] with position discrimination techniques such as optical time-domain reflectometry [11] (OTDR). So far, distributed sensing has mostly been represented by implementations based on Brillouin or Raman backscattering. Brillouin backscattering based techniques have reported dynamic strain sensitivities of ~50×10^{-9} ε/√Hz , for very short polarization-maintaining (PM) fibers (5 meters) [12]. The requirement of averaging successive

Manuscript received Month xx, xxxx; revised Month xx, xxxx; accepted Month xx, xxxx. Date of publication Month xx, xxxx; date of current version Mont xx, xxxx.This work was supported in part by: The European Research Council through project U-FINE (Grant 307441); ITN-FINESSE, funded by the European Union's Horizon 2020 research and innovation program under the Marie-Sklodowska-Curie Action grant agreement nº 722509; the DOMINO Water JPI project, under the WaterWorks2014 cofounded call by EC Horizon 2020 and Spanish MINECO PCIN-2015-219; the Spanish MINECO through the Project TEC2015-71127-C2-2-R; and the regional program SINFOTON-CM: S2013/MIT-2790. The work of LC was supported by EU funding through the project MSCA-ITN-ETN-722509. The work of SML and MRFR was supported by the Spanish MINECO through a "Ramón y Cajal" and "Juan de la Cierva" contracts, respectively.

L. Costa (e-mail: luis.duarte@uah.es), H. F. Martins (e-mail: h.fidalgo@uah.es), S. Martín-López (e-mail: sonia.martinlo@uah.es), M. R. Fernández-Ruiz (email: rosario.fernandezr@uah.es) and M. González-Herráez (email: miguel.gonzalezh@uah.es) are with the Departamento de Electrónica, Universidad de Alcalá, Edificio Politécnico Superior, 28805, Alcalá de Henares, Spain.

This article has been accepted for publication in a future issue of this journal, but has not been fully edited. Content may change prior to final publication. Citation information: DOI 10.1109/JLT.2019.2904560, Journal of Lightwave Technology

measurements, however, severely limits the potential of these techniques for fast and dynamic measurements.

The demand for fast distributed acoustic sensing (DAS) over long ranges, for applications such as non-destructive evaluation of large structures, early detection of damage or surrounding environmental activity, or detection of intrusions over large perimeters, has propelled a recent trend of renewed interest towards Rayleigh-based techniques [7], [13], [14], particularly phase-sensitive (φ)OTDR. Since this technique avoids the need for the previously mentioned averaging due to the moderately high SNR achievable using single-shot data, the sampling rate is ultimately limited by the time-of-flight of the light signal inside the fiber, thus allowing sampling rates as high as 1 kHz for lengths as large as 100 km. Although extremely powerful, conventional schemes of φOTDR present important shortcomings, i.e., they are severely limited by power trace fading points and fail in providing even SNR along the sensing fiber. Recently, a novel interrogation method has been proposed by Pastor-Graells et al. [15], which addresses both problems in a conventional single-mode fiber with minimal alterations to the conventional setup, i.e., by simply introducing a linear chirp to the propagated light pulse.

Here, we extend the work done in [16], developing and formalizing a full derivation of the performance lower bound of chirped pulse φOTDR. This is, to our knowledge, the first proposal of a sensitivity performance lower bound of an fiber optic distributed sensor. We show that, after previously developed first-order phase noise and instrument jitter compensation techniques [17], the main impediment to reach an optimal performance in the technique is related to sampling error, which may easily be addressed by reconstructing the signal through Whittaker-Shannon (sinc) interpolation [18]. The system is then fundamentally limited by the performance of the employed estimator when there is unavoidable additive noise in the signal, which is bounded by the Cramér-Rao Lower Bound (CRLB) for the type of signals acquired with this method [19]–[21]. The proposed model is numerically validated by a series of simulations. We then apply the described strategy experimentally, practically achieving what is, to our best knowledge, unparalleled sensitivity for a distributed optical fiber strain sensor (~10^{-12} ε/√Hz), up to the kHz frequency range. The result obtained reports an improvement of 2 orders of magnitude in strain sensitivity and one order of magnitude in distance range over the performance reported using other techniques, while ensuring a constant value of sensitivity along the length (unlike phase-measuring schemes [22]). It is important to point out that the presented performance has been achieved with significantly less cumbersome stabilization loops than previous short-gauge point-sensor implementations [1], [2] while achieving the simultaneous interrogation of ~1000 consecutive points along the fiber cable (~10 km of fiber), with a direct detection scheme in a conventional optical fiber.

II. Overview of Phase-Sensitive Reflectometry Implementations

Conventional implementations of φOTDR consist in sending a train of coherent transform-limited probe pulses into the fiber, recovering its noise-like fingerprint, and measuring local changes in amplitude as a response to the applied stimulus. This method, however, fails to deliver a true linear and monotonic relationship with the local stimulus, and given the stochastic nature of the retrieved signal, shows a statistically fluctuating signal-to-noise-ratio (SNR) at each point in the fiber [22]. Indeed, some "fading points" have nearly no visibility, preventing any relevant measurement at those positions. Overall, the sensor is unable to quantify a perturbation, being only able to detect and localize its presence. As an attempt to tackle these problems, there have been considerable efforts to develop new interrogation techniques. A linear relationship to the stimulus may be achieved with single-shot data by retrieving the phase of the measured optical trace using e.g. coherent I/Q detection schemes [13], [14]. Still, the

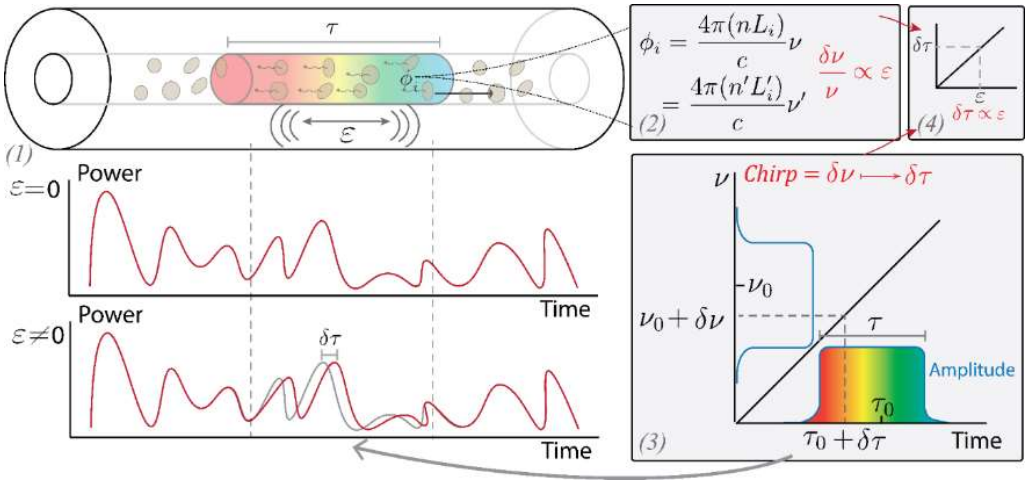

Fig. 1. Working principle of chirped-pulse φOTDR. (1) A coherent probe light pulse is sent into the fiber. Scattering centers within the fiber elastically scatter light, some of which is guided in the opposite direction of the probe-pulse with random amplitude and phase. (2) The resulting optical power from the interference of all the backscattered light components will change as the optical path distance (OPD) is changed locally within the fiber (changes to the refractive index n or length L_i) due to an applied perturbation. A frequency detuning may be used to compensate the change in OPD, thus recovering the previous optical power. (3) Introducing a linear chirp effectively maps this frequency detuning to delay within the pulse window, so the optical power is recovered as a (4) time delay proportional to the perturbation.

This article has been accepted for publication in a future issue of this journal, but has not been fully edited. Content may change prior to final publication. Citation information: DOI 10.1109/JLT.2019.2904560, Journal of Lightwave Technology

implementation is rather cumbersome, as it adds complexity to the simple design of the conventional method, while retaining the problem of "fading points" and uneven SNR [22]. In addition, while it is known that the phase-measuring technique is extremely sensitive to minute values of strain, no rigorous value of strain sensitivity has been given for these sensors, as the uneven nature of the SNR makes it impossible to define a unique sensitivity value along the whole fiber length. Recent wavelength-scanning approaches [23] have been developed, reaching ~100×10^{-12} ε/√Hz sensitivity, using Rayleigh based techniques for a 0.5km long fiber, at a limit of 2 kHz sampling-rate, with 5 m spatial resolution. Through phase detection, pε/√Hz levels have been reached in fibers with ultra-weak gratings [24], as a quasi-distributed approach, though this value remains unattained for standard, readily available single-mode fiber in a fully distributed fashion.

On the other hand, chirped-pulse φOTDR [15] employs a linearly chirped pulse as probe signal. If the bandwidth of this chirped-pulse is much larger than the transform-limited pulse bandwidth, any local change in the fiber optical path (e.g. strain or temperature induced) will translate into a local time shift at the corresponding power trace position (see figure 1).

Consequently, the measurement is converted into a time-delay estimation (TDE) problem, in which the fading points have a minor impact. Thus, unlike the phase-measuring schemes, this technique ensures a consistent value of sensitivity along the length regardless of the fading points [25], which makes it extremely appealing for applications demanding similar measuring quality in all the points along the interrogated fiber. Still, the effects of the different noise sources on the signal-to-noise ratio (SNR) of the retrieved strain signal should be evaluated, and a sensitivity limit should be rigorously explored. The TDE problem has been extensively studied in fields such as radar/sonar [26] and ultrasound elastography [27]. In these other problems the conventionally employed estimator of time-delay consists in determining the lag corresponding to the maximum of the cross-correlation function [19], [20], [28]–[30]. This method, though computationally demanding, offers distinct advantages in computation time over other time-delay estimation alternatives due to its ability to be computed in the frequency domain by exploiting the convolution theorem. Still, the fundamental performance limits of this estimator as a function of φOTDR parameters (pulse width, chirp bandwidth, signal to noise ratio, sampling rate), are still to be determined. In the remainder of this work, we provide the analytical derivation of the performance lower bound of the chirped pulse φOTDR technique, together with the numerical and experimental verification of the presented analysis.

III. Theoretical Model

A. The TDE problem in chirped-pulse φOTDR

φOTDR consists in sending a train of successive coherent light pulses into the fiber and retrieving the backscattered light, thus acquiring a series of successive $x_{meas}(t,i)$ signals for each successive *i*-th laser pulse. Each trace constitutes a noise-like "fingerprint" along the total length of the fiber under test (FUT), where the time-of-flight of the retrieved light, t, can be correlated to the position in the fiber as $z = ct/2n$, c being the speed of light in vacuum and n the refractive index of the fiber. A measurement is then obtained by comparing the "fingerprint" acquired at a specific instant, to a reference fingerprint obtained at a previous one (usually the first shot, *i=0*). Employing a chirped-pulse in φOTDR effectively maps a strain change in the optical fiber into a local delay in the trace pattern, fundamentally converting the interrogation into a local TDE problem. This may be formalized as the measurement of the true delay *D(i)* between sections of two traces (a measurement trace, and a reference trace), each consisting of a section of the complete power trace measured at different times.

$$\begin{aligned} x_{meas}(t,i) &= s(t - D(i)) + n(t,i) \\ x_{ref}(t) &= x_{meas}(t,0), \quad D(0) = 0 \end{aligned} \tag{1}$$

$s(t)$ and $n(t,i)$ being the signal and noise portions of each individual optical trace acquired.

An estimation of the true delay, $\hat{D}(i)$, can be obtained by finding the delay corresponding to the maximum of the cross-correlation between the two sections, enabling fast computation in the spectral domain through the convolution theorem. For the fiber position limited between T_1 and T_2, this can be defined as follows:

$$\begin{aligned} R(\tau,i) &= \int_{T_1}^{T_2} x_{meas}(t,i)\,x_{ref}(t+\tau)\,dt \\ &= R_{ss} * h(t - D(i)) + R_{sn2} + R_{sn1} + R_{n1n2} \end{aligned} \tag{2}$$

$$\hat{D}(i) = \arg\max R(\tau,i) \tag{3}$$

Where $R_{xy}(\tau,i)$ (τ is the lag) is the cross-correlation function (R_{ss} being the signal's autocorrelation function). The correlation time window $T = T_2 - T_1$ defines the spatial resolution of the measurement, though it is ultimately limited by the pulse width: it can be shown that each measured point t' results from the interference of light from all scatterers within the fiber length covered by the pulse surrounding $z = ct'/2n$. Thus, any local change to the local optical paths will influence the backscatter signal measured at that point. Since the SNR is maximized by employing the largest possible pulse for a given spatial resolution, the optimal resolution is achieved when $T = \tau_{pulse}$. Note that effective TDE using cross-correlation requires a well-conditioned signal. A minimum correlation length is required with respect to the trace bandwidth ($T >> 1/B$, B being the chirp bandwidth) [30], the SNR should not be very low, and the signals should be highly correlated. These three conditions are generally fulfilled when measuring dynamic perturbations in chirped-pulse φOTDR.

Under the aforementioned assumptions, the maximum strain measurement performance implies the determination of the mean-square-error lower bound for the TDE problem, under the effects of additive noise in detection. For the moment, we will consider that all other sources of error are negligible in the system. The CRLB for TDE gives a lower bound on the mean-square error for any minimum variance unbiased system [19],

This article has been accepted for publication in a future issue of this journal, but has not been fully edited. Content may change prior to final publication. Citation information: DOI 10.1109/JLT.2019.2904560, Journal of Lightwave Technology

[20], [29]. Determining a CRLB for our system is in many ways analogous to standard radar and sonar postulations, though it demands a detailed look at (2). Assuming relatively high optical SNR, the convolution term of both noises in (2) $R_{n_1 n_2} = n(t,0) * n(t,i)$ may be neglected. The resulting noise influence is due to the convolution of the signal with the noises in the reference and measurement traces. Unlike standard postulations, however, despite having noise in both the reference and measurement signals, the noise in the reference remains constant for each successive measurement. As such, in variance, the system actually performs analogously to an active detection system (no noise in the reference) [19], with a systematic error in the acoustic measurement due to the term R_{sn_1}.

Quazi et al. [19] derived the lower bound for TDE under high and low SNR conditions, for bandlimited active and passive systems, with a constant noise and signal spectrum. The photodetected Rayleigh backscattered spectrum in a typical chirped-pulse φOTDR is triangle-shaped (corresponding to a rectangular-shaped linearly chirped pulse in the temporal domain), while the noise is constant across the whole detected band. Since noise outside the signal bandwidth can be easily filtered during detection, we can determine the CRLB for a triangle shaped (from –B to B) signal spectrum and constant noise (from –B to B), by adapting to this case the derivation done by Quazi et al. (see the Appendix), as

$$\sigma_{CRLB}^2 = \frac{3}{4\pi^2 T}\frac{1}{B^3}\frac{1}{SNR} \tag{4}$$

For a standard single-mode fiber, the rate of strain change per measured time-shift of the φOTDR is related to the chirp bandwidth and pulse duration as [15]

$$\delta\varepsilon / \delta t = \frac{B}{(-0.78)\tau_{pulse}\nu_0} \tag{5}$$

Where ν_0 is the center frequency of the laser probe pulse. Assuming an optimal resolution by making, $\tau_{pulse} = T$, the lower bound for a strain measurement becomes

$$\sigma_{CRLB\varepsilon}^2 = \sigma_{CRLB}^2 (\delta\varepsilon/\delta\tau)^2 = \frac{3}{((-0.78)2\pi)^2}\frac{1}{SNR}\frac{1}{\nu_0 B}\frac{1}{T^3} \tag{6}$$

From this equation, we fully determine the lower bound for the strain determination error as a function of the acquired trace bandwidth, SNR and the correlation window size. These parameters are not independent, however, as the total energy of the retrieved signal is proportional to the pulse width, which translates to increased SNR. Conversely, the total noise energy will scale in proportion to the bandwidth.

It should be instructive to think how the performance will be affected as a function of independent properties of the input probe pulse and test fiber. The signal energy at any position in the fiber may be determined as

$$\boldsymbol{S} = P_{MI}\sigma_{BS}\tau_{pulse}\exp(-2\alpha z) \tag{7}$$

Assuming the peak power is set to the maximum one can use without reaching the onset of modulation instability [31], P_{MI}, the measured signal power then becomes a function of the backscatter coefficient of the optical fiber ($\sigma_{BS} \cong -82$ dB/ns @ 1550 nm, for a standard SMF-28), the pulse width, and the total traveled length of the pulse in the fiber, where $\exp(-2\alpha z)$ is the intrinsic loss from propagation of the retrieved light, for each position in the fiber, taking into account the full roundtrip [32].

Furthermore, considering a spectrally flat additive noise in detection across the full signal bandwidth *B*, of some noise spectral density η_T, the noise energy is given by

$$\boldsymbol{N} = \eta_T B \tag{8}$$

From (7) and (8), we can estimate the SNR as

$$\frac{\boldsymbol{S}}{\boldsymbol{N}} = \left(\frac{P_{MI}\sigma_{BS}}{\eta_T}\right)\frac{\tau_{pulse}}{B}\exp(-2\alpha z) \tag{9}$$

And thus, we can re-write (6) as a function of the probe pulse and input fiber parameters

$$\sigma_{CRLB\varepsilon} = \sqrt{\frac{\eta_T}{P_{MI}\sigma_{BS}}}\frac{\sqrt{3}}{((0.78)2\pi)}\frac{1}{\nu_0}\left(\frac{1}{\tau_{pulse}}\right)^2\exp(\alpha z) \tag{10}$$

Where $\exp(\alpha z)$ can be considered constant for a small enough length of fiber, consisting of the measured correlation window.

At a given acoustic detection bandwidth (of half the laser repetition rate, $f_{acq}/2$) the lower bound for TDE of dynamic strain measurements is expected at $\sigma_{CRLB_\varepsilon}/\sqrt{f_{acq}/2}$ $\varepsilon/\sqrt{\text{Hz}}$. Note that the laser repetition rate is only limited by the total time-of-flight of the pulse in the fiber (1kHz ~ 100 km).

Plugging in the following conventional numbers into the above expression (10): $P_{MI} = 200$ mW, $\tau_p = 100$ ns and noise density estimated as Johnson-Nyquist noise at temperature Θ=300 K across a 50 Ω resistor $\eta_T = 4k_B\Theta R$ (k_B being the Boltzmann constant), we end up obtaining that sensitivities of ~10^{-12} ε/√Hz at 10 kHz laser repetition rate (10 km fiber length) could be readily obtained with the settings of most of the developed chirped-pulse φOTDR implementations published to date. However, other limitations, not considered in the CRLB limit, have hampered achieving this performance up to now. To reach the CRLB limit of performance, we need to ensure that we remove all other sources of error: in this case, sampling error and the effect of phase noise or instrument jitter. Phase-noise and jitter are perceived as a time delay propagated through the whole fiber and thus contribute directly as noise in the acquired acoustic signal. These sources are fully spatially correlated over the whole interrogated length, and thus can be cancelled (to first order) by using an unperturbed section of the fiber to measure the jitter and phase noise, and then compensate any influence in the strain measurements in perturbed sections of the fiber [17].

In addition, when dealing with discrete signals, even in infinite SNR, an error of half the sampling period remains as sampling error. Several methods have been employed in TDE literature to achieve sub-sample accuracy, though some considerations are important to prevent biasing the measurement. Curve-fitting methods, such as a parabolic fit of the three points surrounding the maximum of the cross-correlation function [29], generally bias the measurement [21]. When opting for such a method, the bias should be negligible

This article has been accepted for publication in a future issue of this journal, but has not been fully edited. Content may change prior to final publication. Citation information: DOI 10.1109/JLT.2019.2904560, Journal of Lightwave Technology

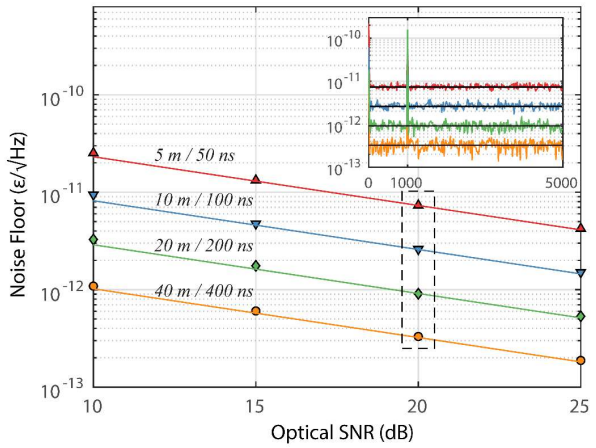

Fig. 2. Noise floors of simulated data and the respective calculated CRLB, for different correlation window sizes and optical trace SNR, using a 1 GHz chirp bandwidth. Inset plot shows the one-sided strain spectral density for the measurements at 20 dB optical SNR. Lines represent the calculated CRLB, points represent the results from simulated data.

when compared to other error sources by oversampling the signal adequately. An alternative way of reducing the sampling error in bandlimited signals, while avoiding the introduction of bias, is by reconstructing the signal through Whittaker-Shannon (sinc) interpolation. This results directly from the Nyquist theorem, so that assuming adequate sampling (i.e. fulfilling the Nyquist criterion), any infinite or periodic discrete signal can be perfectly and unbiasedly reconstructed at higher sampling rates. Though aperiodic and finite signals face small time-domain ringing errors due to Gibbs' phenomenon [33], [34], these are easily addressed by having a large enough correlation window.

B. *Numerical verification of the lower-bound*

The validity of the lower bound determined in (6) was tested using simulated data, so parameters can be tuned independently. A section of 400 m of fiber, sampled at 10 GS/s, was simulated with a 1 kHz sinusoidal variation of refractive index corresponding to an amplitude of 1 nε, according to the relation $\Delta n / n = \Delta \nu / \nu \cong -0.78 \Delta \varepsilon$ [7]. Each acquisition was made at 10 kHz (corresponding to a distance range limit of 10 km of fiber) for a total integration time of 0.05 s (500 laser pulses).

The signal was corrupted with additive, spectrally flat Gaussian noise across the signal bandwidth to reach the desired SNR. Each obtained cross-correlation is reconstructed at a 1000 times higher sampling, by bandlimited interpolation through zero-padding in the frequency domain [35], [36]. Phase noise was not considered for the simulation, since the proposed lower bound assumes an additive noise-limited system. In the presented cases, the SNR is kept relatively high and the signal bandwidth is kept large enough with respect to the correlation time window to consider a negligible probability of anomalous estimates. Figure 2 shows the effects of different chirp bandwidths for different values of (high) signal-to-noise-ratio. It can be seen that there is generally a good agreement between the simulated limit and the one obtained through (6). One can verify that for the lowest considered SNR (10 dB), the obtained sensitivity starts to show some small deviation from the calculated CRLB. For cases of poor SNR, alternative lower bounds have been proposed in the literature [30]. Though the SNR is made to be constant in the simulations, in general, an increase in bandwidth in a real system would influence the amount of additive noise, translating into worse SNR.

The inset of figure 2 represents the impact on performance of changing the spatial resolution of the system (correlation window length and pulse width). In this case, the SNR was forced to be the same for all measurements, though in a real implementation, a longer probe pulse would entail more signal energy, and as such better SNR. As it is visible, the pulse length has a major impact in the performance, improving substantially the sensitivity as the resolution is worsened. However, it should

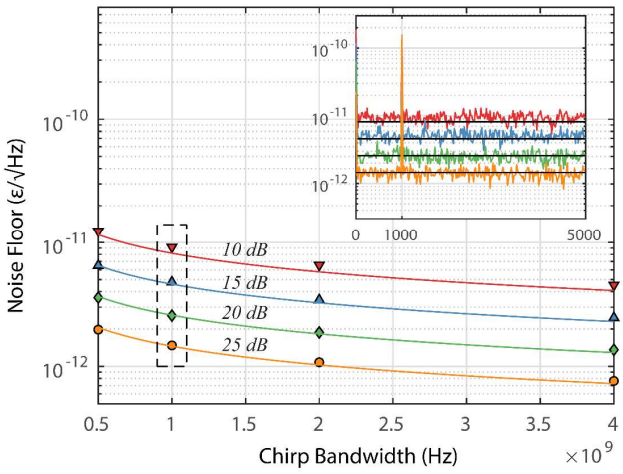

Fig. 3. Noise floors of simulated data and the respective calculated CRLB, for different SNR levels and laser chirp bandwidths, for a 100 ns laser pulse (10 m correlation window). Inset plot shows the one-sided strain spectral density for the measurements at 1 GHz. Lines represent the calculated CRLB, points represent the results from simulated data.

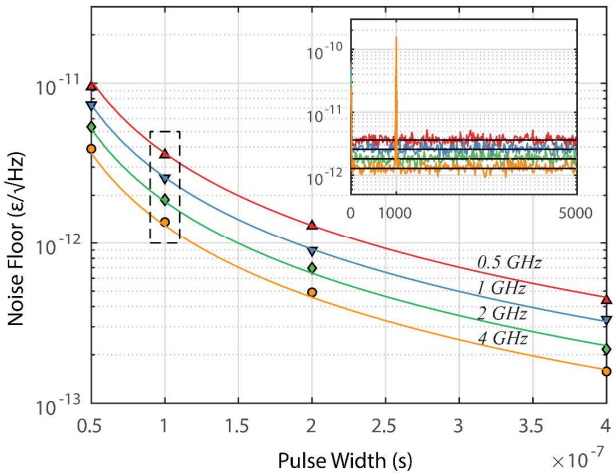

Fig. 4. Noise floors of simulated data and the respective calculated CRLB, for different chirp bandwidths and pulse width/correlation window size, with 20 dB optical SNR. Inset plot shows the one-sided strain spectral density for the measurements at 100 ns pulse width. Lines represent the calculated CRLB, points represent the results from simulated data.

This article has been accepted for publication in a future issue of this journal, but has not been fully edited. Content may change prior to final publication. Citation information: DOI 10.1109/JLT.2019.2904560, Journal of Lightwave Technology

be noted that this is not a major concern in most of the leading applications of this technology (e.g. intrusion detection, seismology), which can afford worsening the resolution at the expense of gaining sensitivity.

Figure 3 represents the strain noise floor for different chirp bandwidths, for different values of optical SNR. As in figure 2, one should keep in mind that in a real system the bandwidth would also influence the amount of thermal noise added to the system, and would thus generally imply worse SNR. In simulation, however, this parameter is controlled independently.

It should be considered that reducing the spectral content also entails additional implications, regarding the physical limitations of φOTDR and cross-correlation. In general, the Cramér-Rao Lower Bound is not achievable with very narrowband signals, and other bounds have been developed for that purpose (such as the Barankin and Ziv-Zakai bounds [37]). For the case of chirped pulse phase-sensitive OTDR, a large bandwidth is intrinsically desired for the frequency-to-time mapping within the optical pulse, as a smaller bandwidth also leads to a faster signal decorrelation as the perturbation increases (since the measured frequency detuning constitutes a larger portion of the total bandwidth of the probe signal). Figure 4 shows the effects of changing the pulse width for different levels of chirp bandwidth, assuming a constant optical SNR. In all simulated cases, there is a very good agreement between the simulation noise floor and the calculated lower bound.

IV. Experimental Results

We tested our model using a conventional φOTDR design, modulating the current of the laser in order to introduce a linear chirp to the pulse, as proposed by Pastor-Graells et al. [15]. The employed setup is depicted in Figure 5.

An external cavity semiconductor laser diode (RIO Planex) working in continuous wave emission at the center wavelength 1550.2 nm, is driven by a current and temperature ILX Lightwave LDC-3724 laser diode controller, with an additional sawtooth-shaped modulation, driven by an Agilent 81150A signal generator. The emitted light is sent through a Thorlabs Semiconductor Optical Amplifier SOA1013SXS (SOA), to be gated as 100 ns light pulses, synchronously to the sawtooth current modulation. Optical isolators were introduced after the laser and SOA to prevent the introduction of any instabilities in the cavities. The resulting pulse is then amplified through an erbium-doped fiber amplifier (EDFA) and filtered to remove amplified spontaneous emission (ASE) noise using a dense wavelength division multiplexer (DWDM). After that, the pulse is sent to the fiber under test through a circulator.

The fiber under test consists of a first section of approximately 200 m, with 20 meters tightly wrapped around a cylindrical piezoelectric actuator, followed by a roll of approximately 1km of fiber, placed within a water bath to prevent unwanted temperature or wind draft induced measurements. The measurements in this piece of fiber are used for first-order phase noise compensation [17]. The compensating fiber is followed by a ~8.7 km roll, for a total interrogation length of ~10 km.

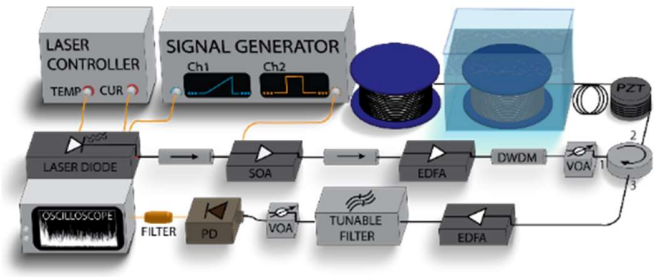

Fig. 5. Experimental setup. Acronyms explained in the text.

The backscattered light is redirected to the detection arm, being first amplified through a second EDFA, then filtered with a tunable filter to mitigate the effect of ASE as much as possible, being finally detected using an 8GHz PDA8GS Thorlabs photodetector. The generated electrical signal is electrically filtered with an analog 900MHz low-pass filter, prior to the digitizer.

Throughout the setup, variable optical attenuators (VOA) are inserted to control the peak power and prevent the onset of non-linear effects during amplification or propagation through the test medium, and to prevent damage to the photodetector. As in the simulated examples, the acquisition was done at 10 GS/s. All the experimental measurements used a 1 GHz bandwidth, 100 ns pulse (10 m correlation window). Calculating the strain sensitivity per sample for the system within the specified parameters yields a sampling error of ±3.3128 nε, which was then reduced 1000 times through interpolation of the cross-correlation function.

The measurements were done for 0.2 seconds, at 10 kHz repetition rate, forcing perturbations with a 300 mV amplitude sine wave applied to the piezoelectric actuator at frequencies from 1 kHz to 4 kHz (10 nε). Laser phase noise and instrument jitter were compensated using the thermally stable section of the fiber [17]. Figs. 6 and 7 show the obtained strain spectra at the output of the system for the two extreme cases of 1 and 4 kHz, in order to show that the processing does not affect the

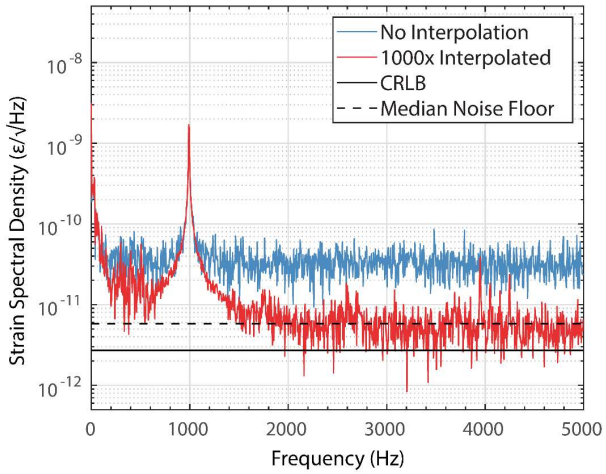

Fig. 6. Strain spectral density from a 0.2 second acquisition with a 1 kHz sinusoidal perturbation. Estimated optical SNR = 19.47 dB. CRLB calculated at 2.715×10^{-12} ε/√Hz median noise floor measured at 5.178×10^{-12} ε/√Hz.

This article has been accepted for publication in a future issue of this journal, but has not been fully edited. Content may change prior to final publication. Citation information: DOI 10.1109/JLT.2019.2904560, Journal of Lightwave Technology

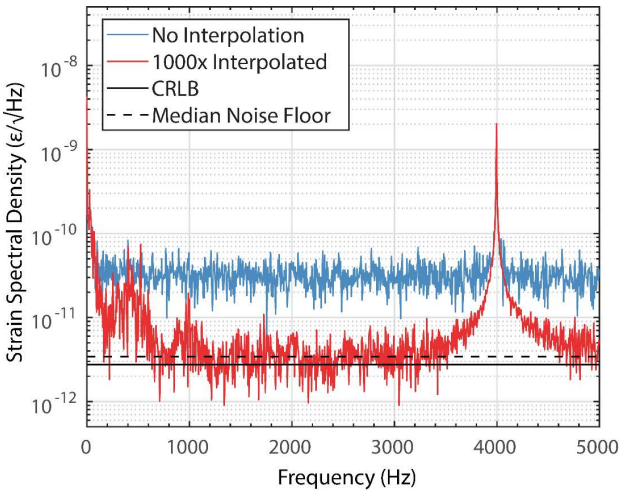

Fig. 7. Strain spectral density from a 0.2 second acquisition with a 4 kHz sinusoidal perturbation. Estimated optical SNR = 19.38 dB. CRLB calculated at 2.744×10^{-12} ε/√Hz median noise floor measured at 3.421×10^{-12} ε/√Hz.

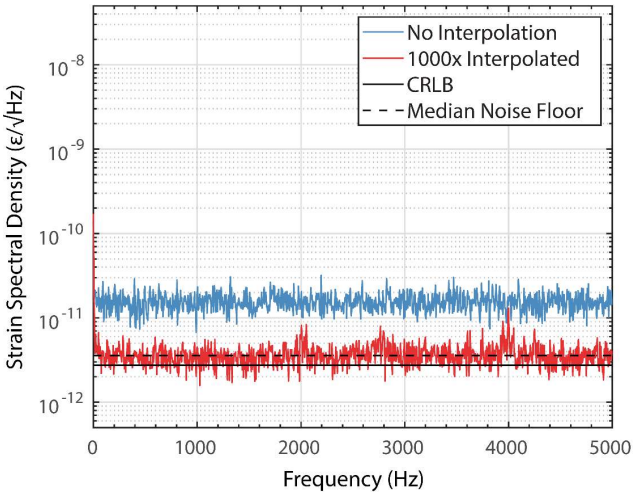

Fig. 8. Strain spectral density from a 0.2 second acquisition in the thermally stable, unperturbed section of the fiber. The data is acquired in the same spool used for phase-noise compensation, outside the region used to measure the phase-noise. The PSDs were averaged over 25 m for better comparison to the lower bound. Estimated optical SNR = 19.62 dB. CRLB calculated at 2.668×10^{-12} ε/√Hz median noise floor measured at 3.590×10^{-12} over the whole frequency range.

frequency response of the system.

In each figure, we represent the proposed CRLB limit (Equation (6).) in a solid black line, with dashed black lines representing the median of the noise floor. It can be observed that after interpolation and phase noise compensation, the noise of our experimental measurements is very close to the one established by the CRLB.

The actual noise limit of our system was measured in an unperturbed zone, in the stabilized section of the fiber, to prevent an increase of the noise floor due to forced convection in the exposed areas of the fiber.

As it is visible in Fig 8, we were able to reach 3.590×10^{-12} ε/√Hz strain sensitivity, versus a calculated lower bound of 2.668×10^{-12} ε/√Hz for an estimated optical trace SNR of 19.62 dB. The slight differences in estimated lower bound and the obtained noise floor could originate from error in the estimation of signal parameters (optical SNR and chirp bandwidth), and due to statistical local variations of the acoustic SNR over time for any given correlation window [25].

V. Discussion and Conclusions

In this study, we have investigated and formalized a lower bound limit on the strain sensitivity performance of chirped pulse phase-sensitive OTDR, considering a given SNR, bandwidth and spatial resolution. The model assumes high SNR and negligible decorrelation between the two measured traces (i.e. relatively small perturbations for the given bandwidth). Further study is required on how the distortion of the optical trace for larger relative frequency detuning affects acoustic measurement performance, as well as on techniques to mitigate the effects of the distortions for large strain, such as smart, periodic updates to the trace reference. Nevertheless, the determined lower bound was found to be in good agreement with simulated data, within the specified assumptions (high SNR, large enough bandwidth compared to window size). To attain such a good agreement, the sampling error has been removed without introducing bias through a Whittaker-Shannon interpolation. Using this interpolation strategy together with laser phase noise compensation allowed us to reach experimentally the proposed lower bound, thus achieving for the first time, to the best of our knowledge, 10^{-12} ε/√Hz sensitivities in distributed strain measurements, in the kHz range and over km-long fibers. This represents several orders of magnitude better strain sensitivity in a distributed sensor than the best previously reported strain measurements published to date. Though the method was designed for distributed strain sensing using chirped-pulse φOTDR, the interpolation techniques used to remove the sampling error, and the determination of the Cramér-Rao Lower Bound can be easily extended to other measurands, such as temperature, pressure or birefringence, and even extended to similar Rayleigh-based sensing techniques more apt for quasi-static strain and temperature measurements, as these commonly employ frequency detuning estimation methods which also rely on cross-correlation, analogous to the problem of TDE [38].

Equation (10) suggests an important trade-off between spatial resolution and acoustic SNR: for a given position on the fiber, it might be reasonable to assume that in order to increase spatial resolution while retaining performance, the SNR should be increased through processing or the onset of non-linear effects in the fiber should be addressed. This motivates research in new ways to improve the signal-to-noise-ratio of the optical trace, to be able to further improve spatial resolution while mitigating the performance decrease. We envisage that this may be achieved through special fibers, such as enhanced backscattering fibers [39], in order to improve the signal power. Available demonstrations in the literature have shown up to ~14dB increase in backscatter coefficient with a relatively small increase in fiber losses [39]. Such a fiber would lead to a ~7dB reduction in the CRLB. Other approaches, such as changes in the pulse shape [40], or pulse compression methods [41] may allow greater input powers without modulation instability. Of course, multi-mode fibers can also be used to avoid

This article has been accepted for publication in a future issue of this journal, but has not been fully edited. Content may change prior to final publication. Citation information: DOI 10.1109/JLT.2019.2904560, Journal of Lightwave Technology

nonlinearities and gain backscatter capture fraction, although such fibers allow covering distances that are much smaller than the ones covered using single-mode fibers.

Although processing speed optimization is out of the scope of this work, it is clear that the processing time required to achieve the extreme interpolation process used in our demonstration is quite heavy. Some improvement may be easily achieved by limiting the maximum perturbation amplitude and interpolating only a smaller region surrounding the peak of the cross correlation, as long as the number of points is enough to make the Gibbs' phenomenon errors negligible. For real-time measurements or applications demanding faster processing, allowing some bias in the measurement of each lag and employing computationally efficient interpolators such as a spectral centroid, or fitting a parabola to the points surrounding the main peak [29] is also a viable option. Cespedes et al. [21] have shown that the error introduced through bias in most curve-fitting methods is relatively small, so even the CRLB retains some usefulness in evaluating the performance in the case of biased estimators. Real-time implementations of the technique may also benefit heavily from hardware multithreading or parallel computing methods, such general-purpose computing on graphics processing units (GPGPU), in order to dramatically increase performance [42]. Parallelization of the chirped-pulse technique should be very efficient and straightforward, as it consists of an "embarrassingly parallel" problem, involving the execution of the same independent processing on all the virtual sensors (or sections of the optical fiber), in which the processing itself also mostly consists of easily parallelized techniques by computing the cross-correlation in the frequency domain through the convolution theorem, taking full advantage of efficient Fast Fourier Transform methods.

The attained sensitivity is approximately only three orders of magnitude higher than the noise induced due to thermal agitations in the optical fiber over a distance equivalent to the pulse resolution [1]. Furthermore, our result was also achieved without the use of ultra-stable lasers unlike the current record-holding attempt for a single short-gauge sensor [1], while simultaneously interrogating as many as ~1000 sensing positions with the same setup, in a time-domain multiplexing technique. We believe that this performance sets a milestone in distributed sensing research.

APPENDIX: FINDING THE CRLB FOR AN ACTIVE SYSTEM WITH THE SPECTRAL CHARACTERISTICS OF CHIRPED-PULSE ΦOTDR

The detected signal in chirped-pulse ϕOTDR shows a bandlimited triangle-shaped spectrum (across the baseband), with approximately constant noise across the same band. Since, in variance, ϕOTDR behaves as an active system, we may follow the derivation done by Quazi et al. [26] for a band-limited active system. The minimum variance for a measurement of delay can be defined as

$$\sigma^2 \geq \frac{1}{d^2 \beta^2} \tag{A1}$$

Where $d^2 = 2E/N_0$, E being the signal energy over some observation time T, with white noise of spectral density $N_0/2$, and β is the root-mean-square bandwidth, in angular frequency, determined as

$$\beta^2 = \frac{\int_{-\infty}^{+\infty} \omega^2 |F(\omega)|^2 \, d\omega}{\int_{-\infty}^{+\infty} |F(\omega)|^2 \, d\omega} = \frac{\int_{-\infty}^{+\infty} (2\pi f)^2 \left(\frac{S_0}{2}\left(1-\frac{f}{B}\right)\right) 2\pi df}{\int_{-\infty}^{+\infty} \left(\frac{S_0}{2}\left(1-\frac{f}{B}\right)\right) 2\pi df} \tag{A2}$$

For a two-sided autospectrum with bandlimited signal spectral power $S(f) = \left(S_0/2\left(1-f/B\right)\right)$ in the range [-*B*,*B*], and 0 outside of the specified bandwidth (i.e. triangle shaped signal spectrum) the root mean square bandwidth can be obtained:

$$\beta^2 = \frac{2(2\pi)^2 \int_0^B f^2 \left(1-\frac{f}{B}\right) df}{2\int_0^B \left(1-\frac{f}{B}\right) df} = \frac{(2\pi)^2 B^2}{6} \tag{A3}$$

So the lower bound becomes

$$\sigma^2 \geq \frac{6N_0}{2E(2\pi)^2 B^2} \tag{A4}$$

Since $E = ST$ and the noise power is $N = N_B B$, assuming constant noise across the signal band, we can rewrite the equation as

$$\sigma^2 \geq \frac{6N_0}{2E(2\pi)^2 B^2} = \frac{3}{4\pi^2 T \, SNR \, B^3} \tag{A5}$$

As shown in (4) in the main text.

REFERENCES

[1] G. Skolianos, A. Arora, M. Bernier, and M. J. F. Digonnet, "Photonics sensing at the thermodynamic limit," *Opt. Lett.*, vol. 42, no. 10, pp. 2018–2021, 2017.

[2] G. Gagliardi, M. Salza, S. Avino, P. Ferraro, and P. De Natale, "Probing the ultimate limit of fiber-optic strain sensing," *Science*, vol. 330, no. 6007, pp. 1081–1084, 2010.

[3] M. Jones, "Structural-health monitoring: A sensitive issue," *Nat. Photonics*, vol. 2, no. 3, pp. 153–154, 2008.

[4] J. P. Dakin, D. J. Pratt, G. W. Bibby, and J. N. Ross, "Distributed optical fibre Raman temperature sensor using a semiconductor light source and detector," *Electron. Lett.*, vol. 21, no. 13, pp. 569–570, 1985.

[5] A. H. Hartog, A. P. Leach, and M. P. Gold, "Distributed temperature sensing in solid-core fibres," *Electron. Lett.*, vol. 21, no. 23, pp. 1061–1062, 1985.

[6] T. Horiguchi, K. Shimizu, T. Kurashima, M. Tateda, and Y. Koyamada, "Development of a distributed sensing technique using Brillouin scattering," *J. Light. Technol.*, vol. 13, no. 7, pp. 1296–1302, 1995.

[7] Y. Koyamada, M. Imahama, K. Kubota, and K. Hogari, "Fiber-optic distributed strain and temperature sensing with very high measurand resolution over long range using coherent OTDR," *J. Light. Technol.*, vol. 27, no. 9, pp. 1142–1146, 2009.

[8] M. Niklès, L. Thévenaz, and P. A. Robert, "Simple distributed fiber sensor based on Brillouin gain spectrum analysis," *Opt. Lett.*, vol. 21, no. 10, pp. 758–760, 1996.

[9] M. E. Froggatt and J. Moore, "High-spatial-resolution distributed strain measurement in optical fiber with rayleigh scatter.," *Appl. Opt.*, vol. 37, no. 10, pp. 1735–40, 1998.

[10] G. P. Agrawal, *Nonlinear fiber optics*, 4th ed. Academic Press, 2001.

[11] K. Aoyama, K. Nakagawa, and T. Itoh, "Optical time domain reflectometry in a single-mode fiber," *IEEE J. Quantum Electron.*, vol. 17, no. 6, pp. 862–868, 1981.

[12] A. Bergman, T. Langer, and M. Tur, "Slope-assisted complementary-correlation optical time-domain analysis of Brillouin dynamic gratings for high sensitivity, high spatial resolution, fast and distributed fiber strain sensing," in *Fifth Asia-Pacific Optical Sensors Conference*, 2015, vol. 96550V, no. July 2015, p. 96550V.

[13] H. F. Martins, K. Shi, B. C. Thomsen, S. Martin-Lopez, M. Gonzalez-Herraez, and S. J. Savory, "Real time dynamic strain monitoring of optical links using the backreflection of live PSK data," *Opt. Express*, vol. 24, no. 19, pp. 22303–22318, 2016.

[14] Z. Wang *et al.*, "Coherent Φ-OTDR based on I/Q demodulation and homodyne detection," *Opt. Express*, vol. 24, no. 2, pp. 853–858, 2016.

[15] J. Pastor-Graells, H. F. Martins, A. Garcia-Ruiz, S. Martin-Lopez, and M. Gonzalez-Herraez, "Single-shot distributed temperature and strain tracking using direct detection phase-sensitive OTDR with chirped pulses," *Opt. Express*, vol. 24, no. 12, pp. 13121–13133, 2016.

[16] L. Costa, H. F. Martins, S. Martin-Lopez, M. R. Fernández-Ruiz, and M. González-Herráez, "Reaching pε/√Hz sensitivity in a distributed optical fiber strain sensor," in *26th Optical Fiber Sensors (OFS) Conference*, 2018, paper number TuD3.

[17] M. R. Fernández-Ruiz, J. Pastor-Graells, H. F. Martins, A. Garcia-Ruiz, S. Martin-Lopez, and M. Gonzalez-Herraez, "Laser Phase-Noise Cancellation in Chirped-Pulse Distributed Acoustic Sensors," *J. Light. Technol.*, vol. 36, no. 4, pp. 979–985, 2018.

[18] T. Schanze, "Sinc interpolation of discrete periodic signals," *IEEE Trans. Signal Process.*, vol. 43, no. 6, pp. 1502–1503, 1995.

[19] A. H. Quazi, "An Overview on the Time Delay Estimate in Active and Passive Systems for Target Localization," *IEEE Trans. Acoust.*, vol. 29, no. 3, pp. 527–533, 1981.

[20] G. C. Carter, "Coherence and time delay estimation," *Proc. IEEE*, vol. 75, no. 2, pp. 236–255, 1987.

[21] I. Céspedes, Y. Huang, J. Ophir, and S. Spratt, "Methods for Estimation of Subsample Time Delays of Digitized Echo Signals," *Ultrason. Imaging*, vol. 17, no. 2, pp. 142–171, 1995.

[22] H. Gabai and A. Eyal, "On the sensitivity of distributed acoustic sensing," *Opt. Lett.*, vol. 41, no. 24, pp. 5648–5651, 2016.

[23] S. Liehr, S. Münzenberger, and K. Krebber, "Wavelength-scanning coherent OTDR for dynamic high strain resolution sensing," *Opt. Express*, vol. 26, no. 8, pp. 10573–10588, 2018.

[24] M. Wu, X. Fan, Q. Liu, and Z. He, "Highly sensitive quasi-distributed fiber-optic acoustic sensing system by interrogating a weak reflector array," *Opt. Lett.*, vol. 43, no. 15, pp. 3594–3597, 2018.

[25] M. R. Fernandez-Ruiz, H. F. Martins, L. D. Costa, S. Martin-Lopez, and M. Gonzalez-Herraez, "Steady-sensitivity distributed acoustic sensors," *J. Light. Technol.*, to be published. DOI: 10.1109/JLT.2018.2877849.

[26] G. C. Carter, "Time Delay Estimation for Passive Sonar Signal Processing," *IEEE Trans. Acoust.*, vol. 29, no. 3, pp. 463–470, 1981.

[27] H. S. Hashemi and H. Rivaz, "Global time-delay estimation in ultrasound elastography," *IEEE Trans. Ultrason. Ferroelectr. Freq. Control*, vol. 64, no. 10, pp. 1625–1636, 2017.

[28] C. H. Knapp and G. C. Carter, "The Generalized Correlation Method for Estimation of Time Delay," *IEEE Trans. Acoust.*, vol. 24, no. 4, pp. 320–327, 1976.

[29] G. Jacovitti and G. Scarano, "Discrete time techniques for time delay estimation," *IEEE Trans. Signal Process.*, vol. 41, no. 2, pp. 525–533, 1993.

[30] J. Ianniello, "Time delay estimation via cross-correlation in the presence of large estimation errors," *IEEE Trans. Acoust.*, vol. 30, no. 6, pp. 998–1003, 1982.

[31] H. F. Martins, P. Corredera, P. Salgado, O. Frazão, S. Martin-Lopez, and M. González-Herráez, "Modulation instability-induced fading in phase-sensitive optical time-domain reflectometry," *Opt. Lett.*, vol. 38, no. 6, pp. 872–874, 2013.

[32] A. Hartog and M. Gold, "On the theory of backscattering in single-mode optical fibers," *J. Light. Technol.*, vol. 2, no. 2, pp. 76–82, 1984.

[33] Y.-C. Jenq, "Sinc interpolation errors in finite data record length," in *10th Anniversary IMTC/94 Advanced Technologies in I & M IEEE IInstrumentation and Measurement Technology Conference*, 1994, pp. 704–707.

[34] J. Selva, "Convolution-based trigonometric interpolation of band-limited signals," *IEEE Trans. Signal Process.*, vol. 56, no. 11, pp. 5465–5477, 2008.

[35] S. V Vaseghi, *Advanced Digital Signal Processing and Noise Reduction*. Wiley, 2008.

[36] J. O. Smith, *Mathematics of the Discrete Fourier Transform (DFT) with Audio Applications*, Second Edi. W3K Publishing, 2007.

[37] S. Reece and D. Nicholson, "Tighter alternatives to the Cramér-Rao lower bound for discrete-time filtering," in *Information Fusion, 2005 8th International Conference on*, 2005, vol. 1, p. 6–pp.

[38] M. A. Soto, X. Lu, H. F. Martins, M. Gonzalez-Herraez, and L. Thévenaz, "Distributed phase birefringence measurements based on polarization correlation in phase-sensitive optical time-domain reflectometers," *Opt. Express*, vol. 23, no. 19, pp. 24923–24936, 2015.

[39] P. S. Westbrook *et al.*, "Kilometer length , low loss enhanced back scattering fiber for distributed sensing," in *2017 25th Optical Fiber Sensors Conference (OFS)*, 2017, pp. 5–8.

[40] M. R. Fernández-Ruiz, H. F. Martins, J. Pastor-Graells, S. Martin-Lopez, and M. Gonzalez-Herraez, "Phase-sensitive OTDR probe pulse shapes robust against modulation-instability fading," *Opt. Lett.*, vol. 41, no. 24, pp. 5756–5759, Dec. 2016.

[41] J. Pastor-Graells *et al.*, "SNR enhancement in high-resolution phase-sensitive OTDR systems using chirped pulse amplification concepts," *Opt. Lett.*, vol. 42, no. 9, p. 1728, 2017.

[42] J. Ghorpade, "GPGPU Processing in CUDA Architecture," *Adv. Comput. An Int. J.*, vol. 3, no. 1, pp. 105–120, 2012.